Available online at www.sciencedirect.com

ScienceDirect

Physics Procedia 67 (2015) 135 – 140

Physics Procedia

25th International Cryogenic Engineering Conference and the International Cryogenic Materials Conference in 2014, ICEC 25–ICMC 2014

Modeling and dynamic simulation of a large scale helium refrigerator

C. Lv[a,c], T.N. Qiu[a,c],J.H. Wu[a,]*, X.J. Xie[b], Q. Li[b]

[a] *Technical Institute of Physics and Chemistry Chinese Academy of Sciences, Beijing 100190, China*

[b] *State Key Laboratory of Technologies in Space Cryogenic Propellants ,Technical Institute of Physics and Chemistry Chinese Academy of Sciences, Beijing 100190, China*

[c] *University of Chinese Academy of Sciences, Beijing 100049, China*

Abstract

In order to simulate the transient behaviors of a newly developed 2kW helium refrigerator, a numerical model of the critical equipment including a screw compressor with variable-frequency drive, plate-fin heat exchangers, a turbine expander, and pneumatic valves was developed. In the simulation, the calculation of the helium thermodynamic properties are based on 32-parameter modified Benedict-Webb-Rubin (MBWR) state equation. The start-up process of the warm compressor station with gas management subsystem, and the cool-down process of cold box in an actual operation, were dynamically simulated. The developed model was verified by comparing the simulated results with the experimental data. Besides, system responses of increasing heat load were simulated. This model can also be used to design and optimize other large scale helium refrigerators.

Peer-review under responsibility of the organizing committee of ICEC 25-ICMC 2014

Keywords: large scale helium refrigerator; modeling; dynamic simulation; system responses; increasing heat load

1. Introduction

Large scale cryogenic systems have been widely used in the scientific field, in chemical industry, in aerospace and so on. Simulation as one of the main ways to study the system performance has important roles, such as process improvement, operator training, and testing of existed/new control strategies. Since 2005, the dynamic simulation

* *Corresponding author. Tel.:* +0-86-010-82543661*; fax:* +0-86-010-82543662
E-mail address: wujihao@mail.ipc.ac.cn

Peer-review under responsibility of the organizing committee of ICEC 25-ICMC 2014
doi:10.1016/j.phpro.2015.06.024

Nomenclature

$\dot{m}$	rate of mass flow (kg/s)	subscripts	
T	temperature (K)	c	compressor
ρ	mass density (kg/m³)	c_{in}	inlet of compressor
P	pressure (Pa)	c_{out}	outlet of compressor
D	diameter (m)	h	heat exchanger
N	speed (rad/s)	h_{in}	inlet of heat exchanger
W	work (W)	h_{out}	outlet of heat exchanger
Cp	mass heat capacity (kJ/kgK)	tur	turbine
h	specific enthalpy (kJ/kg)	tur_{in}	inlet of turbine
η	efficiency	tur_{out}	outlet of turbine

on the cryogenic systems had got fast development. In 2006, Maekawa et al. [1] built a dynamic simulator (C-PREST) using Visual Modeler® (VM®) simulating a 10 kW helium refrigerator/liquefier used in the Large Helical Device (LHD). To enhance the ability to design control algorithm, they[2] implement Matlab® to the C-PREST. Meanwhile, Bradu et al. [3,4] customized EcosimPro® to simulate the 4.5 K helium refrigerator with the CMS magnet and developed a commercial cryogenic library (CRYOLIB) including a set of classic cryogenic equipment. Compared to above simulators, Aspen Hysys® is commercial software of process simulator and has widely operated components codes in petroleum industry. In 2008, C. Deschildre et al. [5] first used it in the simulation of a large scale helium refrigerator and got acceptable results. In order to improve the usability, the details of customization and validation of Aspen Hysys® have been discussed by Rohan Dutta et al. [6]. Although the commercial process simulators are easy in use, it is difficult to debug the process, especially when it is divergent. Therefore, in this paper, a numerical model of a newly developed 2 kW @ 20 K helium refrigerator was developed. Although the dynamic simulation developed quickly in recent years, the simulation on compressor system and the analysis of system responses under different ways of increasing heat load in the references are limited. The start-up of the compressor system was simulated and the system responses of increasing heat load were discussed in the end.

2. Experimental setup of the 2 kW @ 20 K helium refrigerator

The process flow diagram of the 2 kW @ 20 K helium refrigerator is presented in Fig. 1. The process can be divided into two parts: the warm compressor station shown in the dotted lines and the cold box. The warm compressor station with gas manage subsystem is used to guarantee the stability of the system pressure. The low pressure is controlled by the valve (V-1) and the compressor speed. The high pressure is controlled by the discharge valve (V-2) and the charge valve(V-3). When the purity of helium in the compressor system reaches requirement, valves V-7 and V-8 are opened and the cool-down process of the cold box starts. The turbine speed is control by adjusting the opening of V-5.

3. Modeling of the 2 kW @ 20 K helium refrigerator

The accuracy of property data largely influenced the accuracy of simulation results. In the simulation of the 2 kW system, thermodynamic properties of helium are calculated by 32-term modified Benedict-Webb-Rubin (MBWR) state equation [7] which is a widely accepted equation for helium.

3.1. Screw compressors

The screw compressor module was developed based on isentropic process. The difference between the isentropic and the actual work process was corrected by introducing the efficiency. The control strategies have been introduced in section 2.

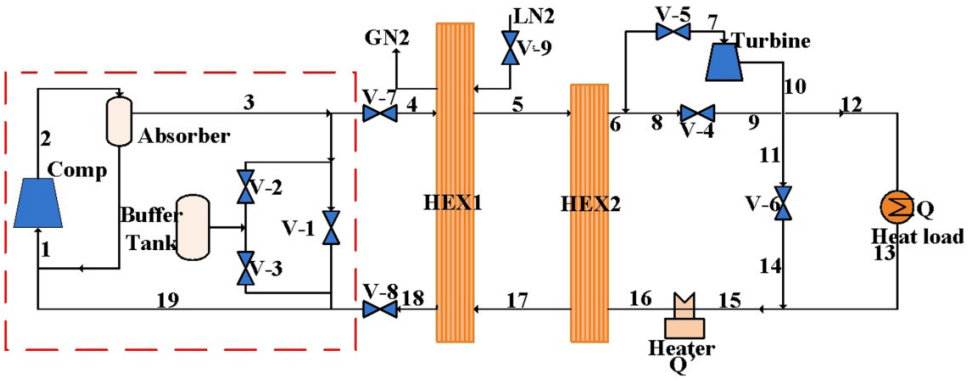

Fig. 1. Process flow diagram of the 2 kW @ 20 K helium refrigerator.

$$\dot{m}_c = \dot{m}_{in} = \dot{m}_{out} = \rho \cdot \dot{V} = \rho \cdot C_n \cdot C_\phi \cdot D_c^{\,2} \cdot L \cdot N_c = \rho \cdot C_n \cdot C_\phi \cdot D_c^{\,2} \cdot L \cdot \frac{f}{\phi}, \tag{1}$$

$$T_{adout} = T_{cin}\left(\frac{p_{cout}}{p_{cin}}\right)^{\frac{\xi-1}{\xi}}, \tag{2}$$

$$W_c = \frac{\dot{m}_c (h_{adout} - h_{cin})}{\eta_s} = \dot{m}_c (h_{cout} - h_{cin}). \tag{3}$$

Where, T_{adout} is the outlet temperature of the isentropic process. η_s is the isentropic efficiency. Φ is the pole pairs of motor, f is the compressor frequency, L is the rotor length, ζ is the specific heat ratio of helium.

Besides, an oil cooler was added to cool the outlet gas. The outlet temperature of the compressor is computed by

$$T'_{out} = \frac{\dot{m}_c C_{pc} T_{cout} - \dot{m}_{oil} C_{poil} (T_{oil}^{out} - T_{oil}^{in})}{\dot{m}_c C_{pc}}. \tag{4}$$

3.2. Heat exchangers

Lumped parameter models of plate-fin heat exchangers are established with a constant wall-temperature assumption. Configurations of HEX1 and HEX2 are listed in Table 1. The following mass and energy balances between the hot and the cold fluid are performed in the equations:

$$\frac{d\dot{m}_h}{dt} = \dot{m}_{h_{in}} - \dot{m}_{h_{out}}, \tag{5}$$

$$\dot{m}_{h_{in}} h_{h_{in}} - \dot{m}_{h_{out}} h_{h_{out}} + kA\Delta T = \rho_h V \frac{dh_{h_{out}}}{dt}. \tag{6}$$

Where V is the control volume of heat exchanger, A is the heat transfer area, k is heat transfer coefficient, $k = \rho\, v_{vel}\, St\, C_{ph}$. St can be calculated by $St = \frac{j}{Pr^{2/3}}$[8], j is the dimensionless heat transfer coefficient, and can be

provided by manufacture. v_{vel} is the velocity of fluid.

3.3. Turbine expanders

Isentropic process is also used in the calculation of the turbine, in addition, equations of capacity and isentropic efficiency are also needed which can be fitted by experimental data:

$$capacity = k_o \frac{P_{tur_{in}}}{\rho_{tur_{in}} \sqrt{Z_{tur_{in}} T_{tur_{in}}}}, \tag{7}$$

$$\eta_{tur} = \mathrm{a+b}\left(\frac{U_1}{C_0}\right) + c\left(\frac{U_1}{C_0}\right)^2, \tag{8}$$

where, $Z_{tur_{in}}$ is the compressibility factor of inlet stream of turbine. U_1 is the tip speed of impeller, $U_1 = \pi D_{tur} N_{tur}$. C_0 is the adiabatic speed. The coefficients of k_o, a, b, c were determined by experimental data.

The speed is calculated as[3]:

$$I \cdot N_{tur} \cdot \frac{\mathrm{d}N_{tur}}{dt} = W_{tur} - W_{turd} \cdot \left(\frac{N_{tur}}{N_d}\right)^4, \tag{9}$$

where, I is the inertia momentum of the shaft. N_d, W_{turd} are rated speed, rated power of turbine. The rotor wheel diameter and rated shaft speed are presented in Table 1.

3.4. Valves

Pneumatic valves are calculated by Cv and the opening [9] with the assumption that mass enthalpy of inlet is equal to that of outlet. Cv is obtained from producer and presented in Table 1.

Table 1. Specification of critical equipment.

Equipment	Parameter	value
Compressor	Rotor diameter	28 mm
HEX1	Fin geometry (height, thickness, pitch)	6.5 mm,0.3 mm,1.7 mm
	Dimension	1 m x 0.47 m
HEX2	Fin geometry (height, thickness, pitch)	6.5 mm,0.3 mm,1.7 mm
	Dimension	1.8 m x 0.47 m
Turbine	Turbine wheel diameter	35 mm
	Brake wheel diameter	60 mm
	Rated speed	120000 rpm
V-1/2/3/4/5/6	Cv	18/8/11/11/18/69

4. Results and discussion

4.1. Simulation of compressor cycle

When the compressor receives the start-up signal, it runs to 25 Hz in 2 minutes. In the experimental equipments, a KAESER screw compressor with variable frequency drive was used, and relationship of mass flow and the

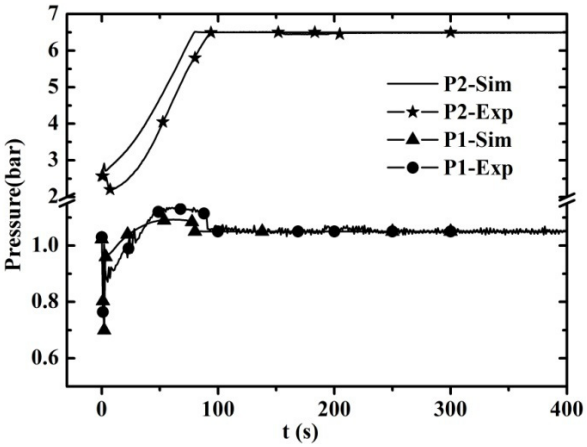

Fig. 2. Variation of low pressure and high pressure versus time.

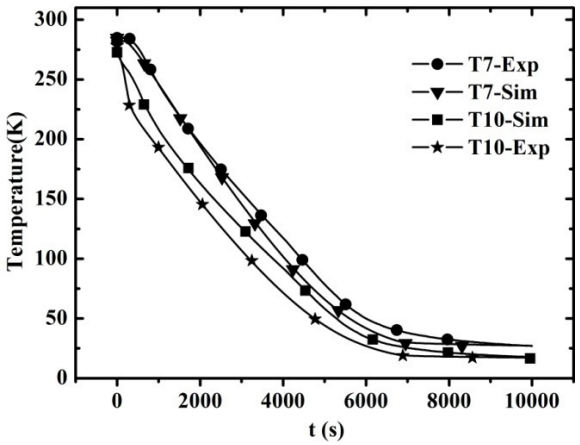

Fig. 3. Variation of inlet and outlet temperature of turbine versus time.

compressor speed was: 46 g/s @ 25 Hz, 110 g/s @ 60 Hz in rated condition. Fig. 2 presented the simulated results compared with the real data obtained during the commissioning in October 2013.

P1 and P2 present the pressure of location of 1 and 2 which are showed in Fig. 1. From the results, it can be observed that the simulation produced acceptable trends during the start-up of the compressor. However, the simulation time was faster than actual operation. The reasons are as follows: i) the time lag of signal transmission is not taken into account in the simulation, ii) the inertia of compressor is unknown. The phenomenon that the low pressure was below atmospheric pressure was observed in initial stage both in actual plant and simulation (see Fig. 2). At this moment, the opening of V-1 was forced to 95% to prevent air contaminant into compressor system.

4.2. Cool-down of cold box

The simulation results of the cool-down process without heat load are presented in Fig. 3. T7 and T10 present the temperature of state 7 and 10 which are shown in Fig. 1. The moment that V-5 started to open in the actual operation was taken as the initial condition in the simulation. From the results, it may be observed that the process takes about 2.5 h to go down to 20 K. The error of cool-down time between simulation and real data was about 10%. However, the temperature deviation still existed. The reasons may be as follows: i) the initial cool-down sequence of cold box is unknown, ii) fitted equations may be more suitable for full load conditions, and the model should be further modified to improve the accuracy of simulation results.

4.3. System responses and analysis of increasing heat load

The heat load in the 2 kW system is created with a heater by manual operation. In the experiment, how to increasing heat load hadn't clear approaches. However, under different ways of increasing heat load from zero to 2 kW, the elapsed time and the thermal disturbances of the system are not the same. Therefore, it is necessary to analyze the system responses of increasing heat load, and find the appropriate way with small disturbances. The operation conditions were set as follows: cases A and B represented the increasing rate of heat load of 0.5 W/s and 0.2 W/s, respectively. Case C was set to maintain T16 (the temperature at the location 16, which was presented in Fig. 1) about 20 K by adjusting the heat load Q.

The elapsed time of cases A, B, C, was 4.17, 4.12 and 3.1 h, respectively. The increasing rate in condition A was fastest (seen in Fig. 4) while the elapsed time was longest. The main reason may be that T16 was away from design temperature (20 K) at initial stage, and decreasing T16 was time consuming. T16 in condition B was in the range of 20 ± 0.5 K, but the time was not shorter. This was because the cooling capacity was larger than heat load at starting stage, and the operating condition of the turbine was in off-rating condition. C was the ideal condition without any

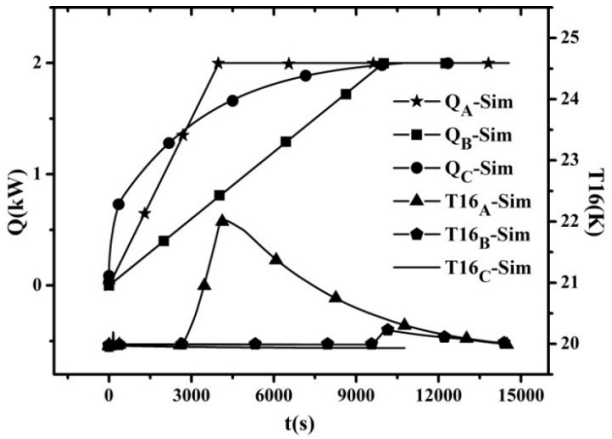

Fig. 4. Variation of T16 and Q versus time.

disturbances, and the corresponding response time was shortest. Compared to C, B was easy to implement and had acceptable thermal disturbances Therefore, in the 2 kW system, it is recommended to use case B in the control of the increasing heat load.

5. Conclusion

The good agreement between the simulation and experiment data allows us to validate the component models. Simulations applied to the different ways of increasing heat load presents that there is a most suitable rate in the actual operation (case B). Further experiments will be performed to verify this simulation result. The model will be further modified and will be checked in a helium liquefier to prove its ability in the near future.

Acknowledgement

This work was supported by the fund of the State Key Laboratory of Technologies in Space Cryogenic Propellants.(SKLTSCP1306).

Reference

1. Maekawa, R., K. Ooba, K. Ando,T. Mito. Dynamic simulation of a large scale cryogenic plant. ADVANCES IN CRYOGENIC ENGINEERING: Transactions of the Cryogenic Engineering Conference-CEC. 2006; 823: 2002-2009.
2. Maekawa, R., S. Takami, K. Oba,M. Nobutoki. Adaptation of advance control to the helium liquefier with C-PREST. 22nd International Cryogenic Engineering Conference. 2008: 243.
3. Bradu, B., P. Gayet,S.-I. Niculescu, A process and control simulator for large scale cryogenic plants. Control Engineering Practice, 2009; 17: 1388-1397.
4. B., B., A. R., B. E., C. P., G. P.,V. A. CRYOLIB：a commercial library for modelling and simulation of cryogenic processes with EcosimPro. Proceedings of ICEC 24-ICMC 2012. 2012: 47-50.
5. Deschildre, C., A. Barraud, P. Bonnay, P. Briend, A. Girard, J.M. Poncet, P. Roussel, S.E. Sequeira, J.G. Weisend, J. Barclay, S. Breon, J. Demko, M. DiPirro, J.P. Kelley, P. Kittel, A. Klebaner, A. Zeller, M. Zagarola, S. Van Sciver, A. Rowe, J. Pfotenhauer, T. Peterson, J. Lock, Dynamic Simulation of an Helium Refrigerator. 2008; 985: 475-482.
6. Dutta, R., P. Ghosh,K. Chowdhury, Customization and validation of a commercial process simulator for dynamic simulation of Helium liquefier. Energy, 2011; 36: 3204-3214.
7. McCarty, R., V. Arp, A new wide range equation of state for helium. Adv. Cryog. Eng, 1990; 35: 1465-1475.
8. Wang S.H. *Plate fin heat exchanger*. 1rd ed. Bei Jing:Chemical Industry Press; 1984.
9. Lu P.W. *Regulating valve practical technology*. 1rd ed. Bei Jing: China Machine Press*;* 2006.